

Cooperation with Kenya – PhD Research CFD Simulation Validation of Wood Combustion in Laboratory Fixed Bed vs. Numerical Reaction Model DEM Approach

Abstract

In this study, numerical simulation of wood combustion in a laboratory fixed bed reactor is presented. The main aim was to test the suitability of CFD-DEM approach in predicting temperature distribution and species generation in a fixed bed reactor. A commercial software code STAR CCM+ was used to simulate combustion of eucalyptus wood under air condition. Lagrange-Euler (CFD-DEM) approach was used in which gas phase was calculated using computational fluid dynamics while solid phase was tracked in lagrange approach. Simulation results were compared to experimental data. A good agreement between simulation results and measured data was achieved. This proved that CFD-DEM method can be used in design and optimization of new equipments.

Experimental Set-Up

A schematic diagram of the experimental set-up used in this work is shown in the Fig. 1. It is a cylindrical chamber with an internal diameter of 40 mm and a height of 200 mm. Air inlet port is located at the bottom and grate is located 40 mm from it. Flue gas outlet is located at the top of the chamber. It has provisions for thermocouple insertions located at equidistant of 10 mm from one another. Internal and external parts are made of stainless steel and between them is a 20 mm thick refractory cement for insulation. The reactor was operated in counter-current flame propagation mode. Oxidizer was supplied from the bottom.

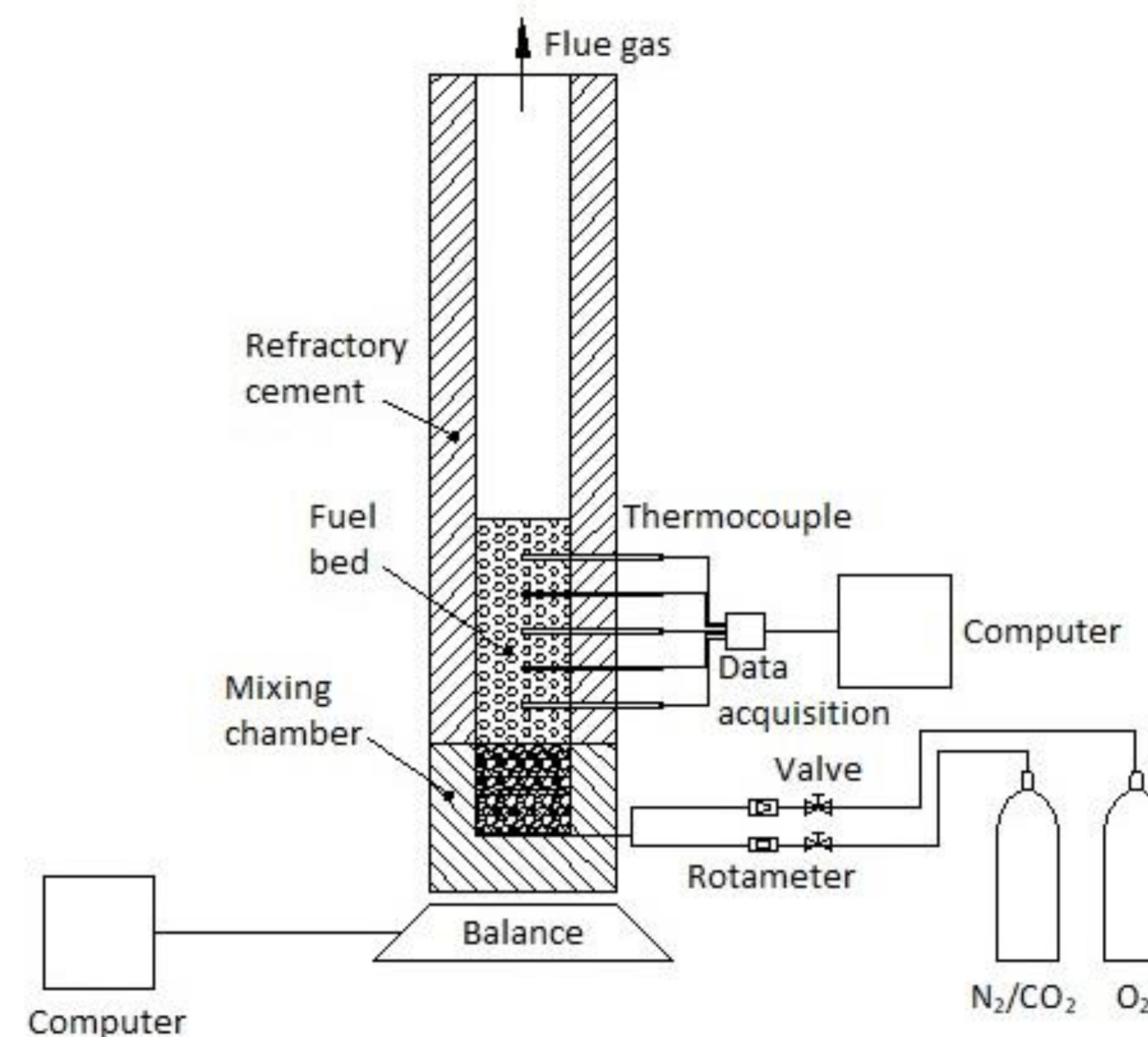


Table 1: Proximate and ultimate analysis of fuel sample

Proximate analysis (wt%)	
Moisture	10.3
Volatile matter (wt% dry basis)	84.9
Fixed carbon (wt% dry basis)	14.9
Ash (wt% dry basis)	0.2
Ultimate analysis (wt% dry basis)	
C	50.87
H	5.73
N	0.3
O (by difference)	43.1
Gross calorific value (MJ/kg)	19.3

Table 2: Biomass kinetic model

Drying		Rate expression	
R(1)	Wet wood \rightarrow Dry wood + $H_2O(g)$	$R_{dry} = Y_{m,pb,wt} 1.6 \times 10^{27} \exp(-25000/T_d)$	
Pyrolysis Reactions		Rate expression, $K_i = A_i \exp(-E_i/RT)$	Kinetics: $A(s^{-1}), E(kJ/mol)$
R(2)	Dry wood \rightarrow gas	$\dot{\omega}_g = K_2 \rho_{b,dry}$	$A_2 = 111 \times 10^9, E_2 = 177$
R(3)	Dry wood \rightarrow Tar	$\dot{\omega}_t = K_3 \rho_{b,dry}$	$A_3 = 9.28 \times 10^9, E_3 = 149$
R(4)	Dry wood \rightarrow char	$\dot{\omega}_c = K_4 \rho_{b,dry}$	$A_4 = 30.5 \times 10^9, E_4 = 125$
R(5)	Tar $\rightarrow Y_t Tar_{inert} + Y_{CO} CO + Y_{CO_2} CO_2 + Y_{H_2} H_2 + Y_{CH_4} CH_4$	$\dot{\omega}_{Tar} = K_5 \rho_{Tar}$	$A_5 = 9.55 \times 10^4, E_5 = 93.37$
Homogeneous Gas-Phase Reactions		Rate expression, $K_i = A_i T^n \exp(-E_i/RT)$	Kinetics: $A(s^{-1}), E(kJ/mol)$
R(6)	$2CO + O_2 \rightarrow 2CO_2$	$R_{CO} = K_6 [CO][O_2]^{0.25} [H_2O]^{0.5}$	$A_6 = 2.24 \times 10^{12}, n = 0, E_6 = 167.36$
R(7)	$CH_4 + 2O_2 \rightarrow CO_2 + 2H_2O$	$R_{CH_4} = K_7 [CH_4]^{0.7} [O_2]^{0.8}$	$A_7 = 11.58 \times 10^{18}, n = 0, E_7 = 202.5$
R(8)	$2H_2 + O_2 \rightarrow 2H_2O$	$R_{H_2} = K_8 [H_2][O_2]$	$A_8 = 2.19 \times 10^9, n = 0, E_8 = 109.2$
R(9)	Tar + $2.9O_2 \rightarrow 6CO + 3.1H_2$	$R_{Tar} = K_9 [tar]^{0.4} [O_2]$	$A_9 = 9.2 \times 10^6, n = 0, E_9 = 80.2$
R(10)	$CO + OH \rightarrow CO_2 + H$	$R_{CO} = K_{10} [CO][OH]$	$A_{10} = 4.76 \times 10^7, n = 1.3, E_{10} = 0.293$
R(11)	$H + O_2 \rightarrow O + OH$	$R_H = K_{11} [O][OH]$	$A_{11} = 2.65 \times 10^{16}, n = -0.671, E_{11} = 71.347$
R(12)	$H_2 + O_2 \rightarrow OH + OH$	$R_{H_2} = K_{12} [H_2][O_2]$	$A_{12} = 2.51 \times 10^{12}, n = 0, E_{12} = 163.075$
R(13)	$H_2O + CO \rightarrow CO_2 + H_2$	$R_{H_2O} = K_{13} [H_2O][CO]$	$A_{13} = 2.78, n = 0, E_{13} = 12.55$
R(14)	$CO_2 + H_2 \rightarrow H_2O + CO$	$R_{CO_2} = K_{14} [CO_2][H_2]$	$A_{14} = 93.69, n = 0, E_{14} = 46.594$
Heterogeneous Reactions		Rate expression, $K_i = A_i \exp(-E_i/RT)$	Kinetics: $A(s^{-1}), E(kJ/mol)$
R(16)	$\Omega C + O_2 \rightarrow 2(\Omega - 1) CO + (2 - \Omega) CO_2$	$\dot{\omega}_{char,O_2} = K_{16} P_{O_2} S_{a,char}$	$A_{16} = 2.54 \times 10^{-8}, E_{16} = 74.8$
R(17)	$C + CO_2 \rightarrow 2CO$	$\dot{\omega}_{char,CO_2} = K_{17} P_{CO_2} S_{a,char}$	$A_{17} = 1.81 \times 10^{-2}, E_{17} = 130$
R(18)	$C + H_2O \rightarrow CO + H_2$	$\dot{\omega}_{char,H_2O} = K_{18} P_{H_2O} S_{a,char}$	$A_{18} = 1.81 \times 10^{-2}, E_{18} = 130$

Fig 1: Schematic diagram of experimental set-up

The model results were validated by comparing predicted and measured temperature at corresponding position in the fuel bed. Shown in Fig. 4 is temperature history at 5 cm from bed bottom. A good agreement between predicted and measured temperature values is achieved. The graph shows that the temperature profile has two peaks. As the flame front passes the position where measurement is done, temperature rises rapidly up to the first peak. Then it decreases to about 900 K. Exothermic reactions of the volatiles increases the temperature while drying and pyrolysis which are endothermic processes decrease the temperature. The second part of the graph where temperature rises signifies that endothermic processes have ended. The volatiles transported from lower part of the bed burn in this region. The last regime where temperature decrease is characterized by char gasification and oxidation.

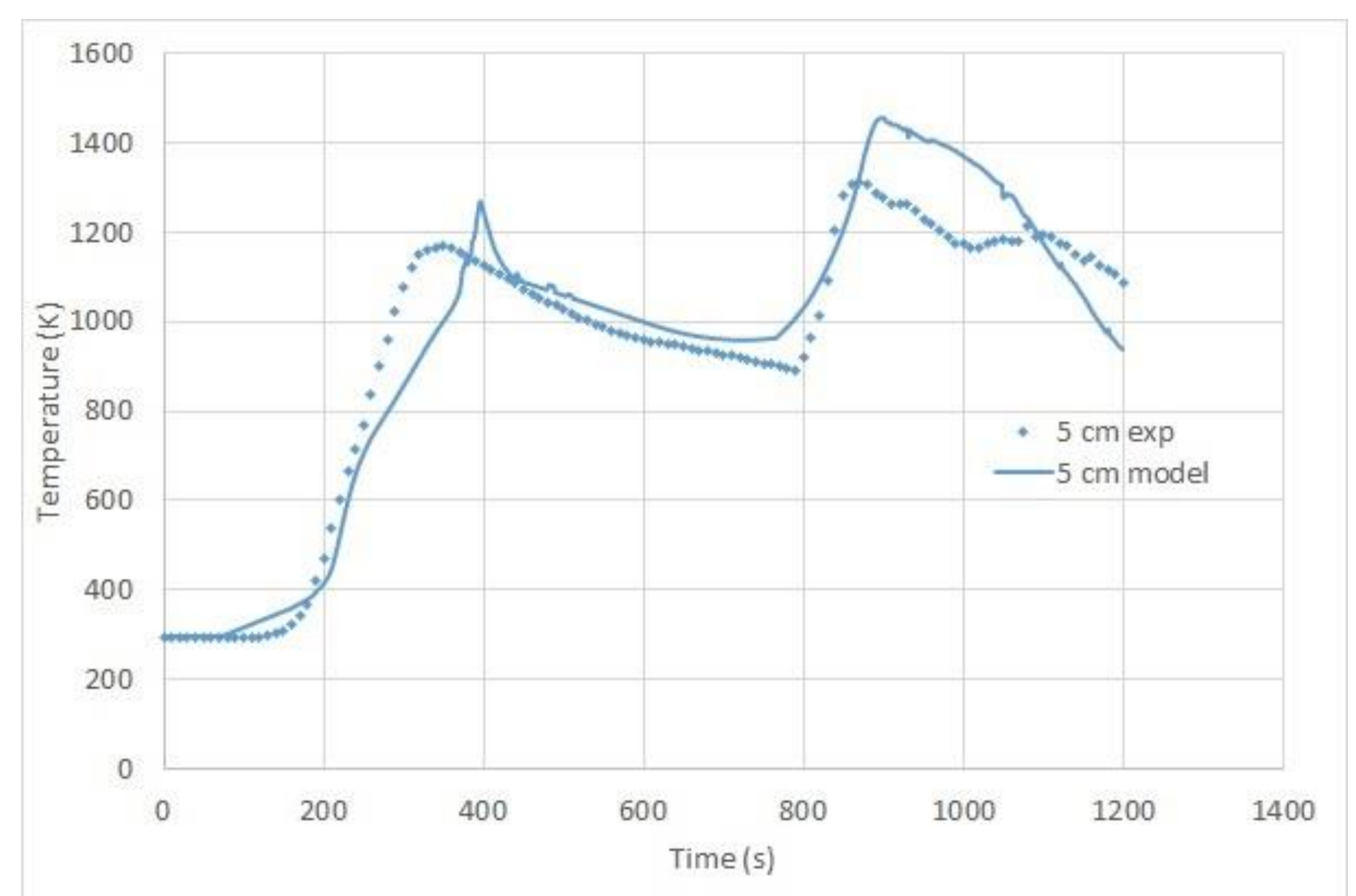
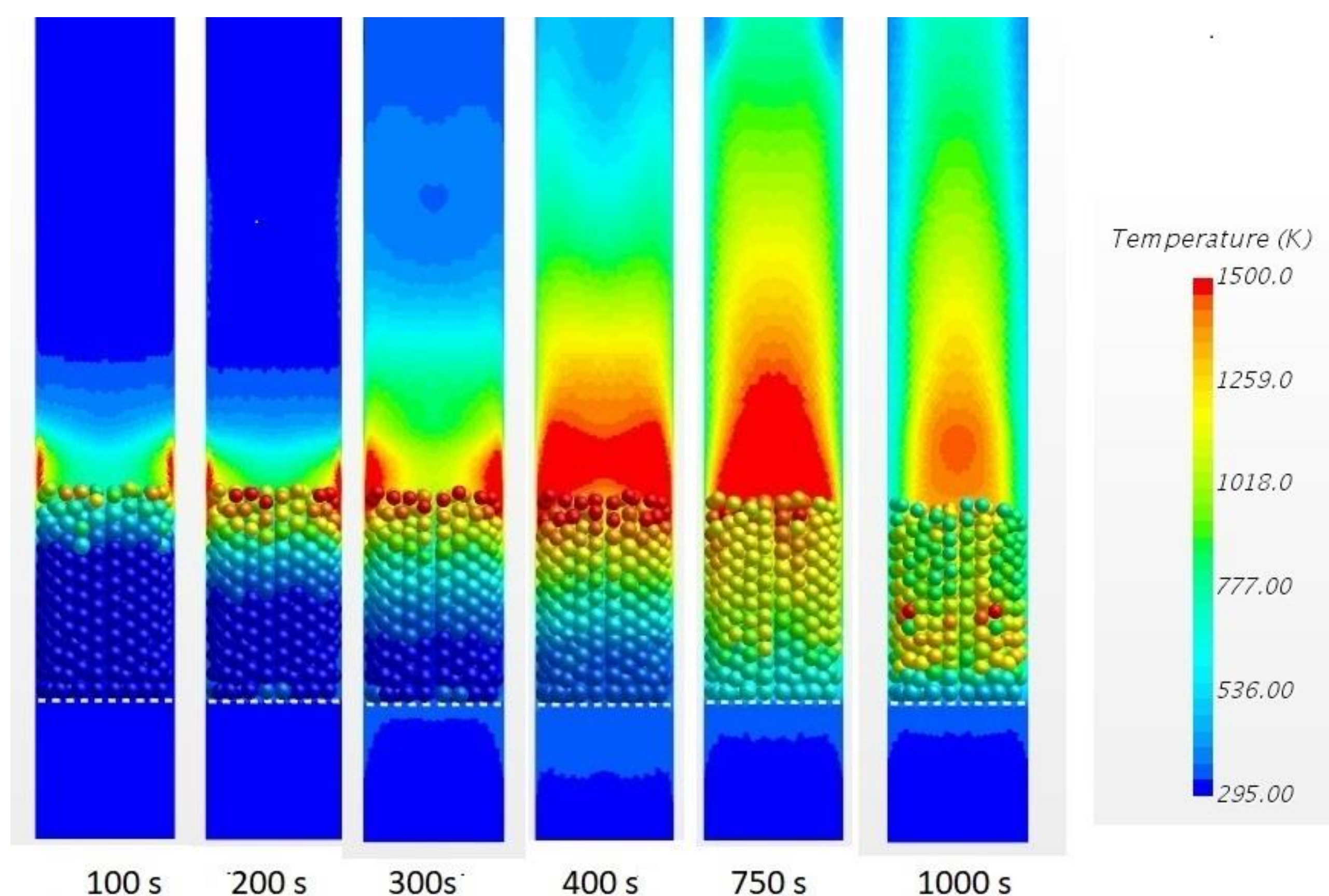


Fig 4: Measured and predicted temperature profile at 5 cm